Sensors and Materials, Vol. 32, No. 7 (2020) 2311–2320
MYU Tokyo

S & M 2260

Estimating Temperature Map in Body–Mattress Contact from a Few Thermostats to Prevent Decubitus

Wen-Hsien Ho,[1,2†] Ching-Ju Hung,[3†] Kao-Shing Hwang,[1,4]
Yenming J. Chen,[5*] and Jinn-Tsong Tsai[6**]

[1]Department of Healthcare Administration and Medical Informatics, Kaohsiung Medical University,
No. 100, Shih-Chuan 1st Road, Kaohsiung 807, Taiwan
[2]Department of Medical Research, Kaohsiung Medical University Hospital,
No. 100, Shih-Chuan 1st Road, Kaohsiung 807, Taiwan
[3]Department of Pharmacy, Yuan's General Hospital, No. 162, Cheng Kung 1st Road, Kaohsiung 802, Taiwan
[4]Department of Electrical Engineering, National Sun Yat-Sen University,
No. 70, Lienhai Road, Kaohsiung 804, Taiwan
[5]Department of Logistics Management, National Kaohsiung University of Science and Technology,
No. 1, University Road, Kaohsiung 824, Taiwan
[6]Department of Computer Science, National Pingtung University,
No. 4-18, Min-Sheng Road, Pingtung 900, Taiwan

(Received April 16, 2019; accepted May 20, 2020)

Keywords: body temperature distribution, unscented Kalman filter, partially observed Markov process, heat flux estimation

Patients who are bedridden for a long time are afflicted with multiple problems. Inactive and bedridden patients under sustained pressure are prone to pressure ulcers. High skin temperature and humidity also induce pressure sores. Thus, using automated assistance to measure contact temperature and humidity is a viable solution. A low-cost monitoring device is desperately needed by institutes to improve the quality of care. We embed a few thermostats inside a mattress and estimate the temperature distribution of the entire body on the contact surface of the mattress. The heat flux and temperature distribution, as well as necessary thermal parameters, can be reversely estimated from the measured temperature trajectories of the embedded thermostats by using heat diffusion equations in the finite difference method and the dual iterative estimation of an unscented Kalman filter. We conduct 1D and 2D experiments in a controlled environment and obtain excellent results. The estimated temperature map and heat flux are accurate for a constant amount of flux. Our algorithm is proven to be pragmatic because our findings show that measurements can be taken without knowing any dimensions or thermal properties of the mattress. This will help to prevent bedridden residents from developing pressure sores.

1. Introduction

The rapid growth of the elderly population has increased the demand for long-term care of people with chronic diseases and dysfunction. In addition to health and medical services,

†Equal contributors.
*Corresponding author: e-mail: yjjchen@nkust.edu.tw
**Corresponding author: e-mail: jttsai@mail.nptu.edu.tw
https://doi.org/10.18494/SAM.2020.2869

disabled people and those without self-care capacity need extensive long-term care services. The demand for long-term care in Taiwan will increase substantially in the future. In addition to the increased number of elderly people, a decline in the youth population is expected. The current nursing labor force is seriously insufficient, and a major gap exists between the supply and demand of the long-term care industry.

Our solution complements the existing commercial care beds by supplementing indirect temperature estimation. The temperature on which we focus is the whole contact surface between the body and the mattress. Given the bodily discomfort caused by placing a thermometer on the bed surface and the difficulty in obtaining the temperature of the entire contact surface to conduct surface measurement, a small number of thermometers are inserted in the center of a mattress to estimate the temperature distribution of the body–mattress contact surface. This requirement is difficult because the mattress and the human body's thermal parameters are unknown, and using unknown parameters to estimate an unknown temperature blindly is challenging.

High skin temperature and humidity also induce pressure sores. Their blood circulation often becomes occlusive due to insufficient body movement. A common solution is to hire helpers to regularly turn patient bodies. Assisting bedridden patients to turn over every 1–2 h is a necessary action to prevent pressure sores. This frequency is determined by the patient's condition, personnel workload, and past experience. However, these factors change dynamically. Turning too often wastes care resources; however, turning less frequently causes decubitus. Thus, using information and communication technology (ICT) in the bed to monitor mattress temperature and humidity is a viable solution.

We embed a few thermostats inside a mattress and estimate the temperature distribution of the entire body on the contact surface of the mattress. The heat flux and temperature distribution, as well as necessary thermal parameters, can be reversely estimated from the measured temperature trajectories of the embedded thermostats by using heat diffusion equations in the finite difference method and the dual iterative estimation of an unscented Kalman filter. From the temperature trajectory of the center of the mattress, we estimate all source variables in reverse, including all thermal parameters, surface heat flux, and the overall temperature distribution of the mattress by using the heat diffusion equation in the finite difference method. Three 1D and 2D experiments are conducted in a controlled environment and promising results are obtained: the temperature distribution map and the source heat flux can be accurately estimated.

Pressure sore monitoring aims to collect and estimate the prevalence rate of pressure sores and analyze the causes to prevent and control pressure sores. The ways of body heat dissipation include through the skin, breathing, excretion, and secretion; skin heat dissipation takes up the highest proportion (approximately 70%). The heat dissipation mode of the skin is mainly related to the amount of blood flow perfusion.

The reverse question has various conceptual issues. We focus on using differential equations to solve biomedical problems. In addressing inverse problems, most adjustment methods can only determine the numerical difficulty from a mathematical aspect, but problems with multiple solutions must be solved by restoring constraints that may be missing. Existing research continues to contribute to the problem that physiological models and patient-specific data

are consistently damaged by noise. Greensite[1] estimated the temporal and spatial common variables under certain mathematical assumptions on the basis of the structure inherent in the space–time correlation matrix. Wang *et al.*[2] constrained the inverse problem of space and time dimensions by constraining the distribution of transmembrane potentials by the diffusion reaction model of cell activation dynamics. They suggested relying on statistical methods to solve model and data errors, namely, prior knowledge of cell current dynamics and evidence of potential surface data.[3] The reverse problems that are difficult to solve require a considerable amount of learning effort and involve time-related statistical techniques. Thus, in this study, the machine learning and generation methods are used in a random process and modeling, that is, system identification or parameter identification in other fields. The Bayesian method is at the heart of various statistical methods. Algorithms based on the Markov chain Monte Carlo (MCMC) method have recently become common for statistical machine learning.[4]

MCMC algorithms are also effective in model estimation and correction. Campillo and Rossi[4] developed a convolutional particle filter for parameter estimation in the general state-space model. Andrieu and co-workers[5,6] reviewed the MCMC algorithm and applied the particle MCMC method to statistical machine learning. Snoek *et al.*[7] also applied Bayesian optimization to machine learning algorithms. Formal statistical algorithms often require a large amount of computational resources; thus, several approximation methods have been proposed. Toni *et al.*[8] developed an approximate Bayesian calculation scheme for parameter inference and model selection. Ionides *et al.*[9] developed an effective parameter estimation algorithm in iterative filtering. They also[10] made substantial improvements in the parameters of the observable part of the observational problem with inference difficulty by improving the convergence of the iterative Bayesian mapping. Tao *et al.*[11] estimated model parameters in an ensemble model. Tang *et al.*[12] studied parameter estimation methods for highly efficient data assimilation.

2. Materials and Methods

We have developed a coordinated central controller, as shown in Fig. 1. We use the partially observed Markov process (POMP) model, a dynamic MCMC model, for a basic computing

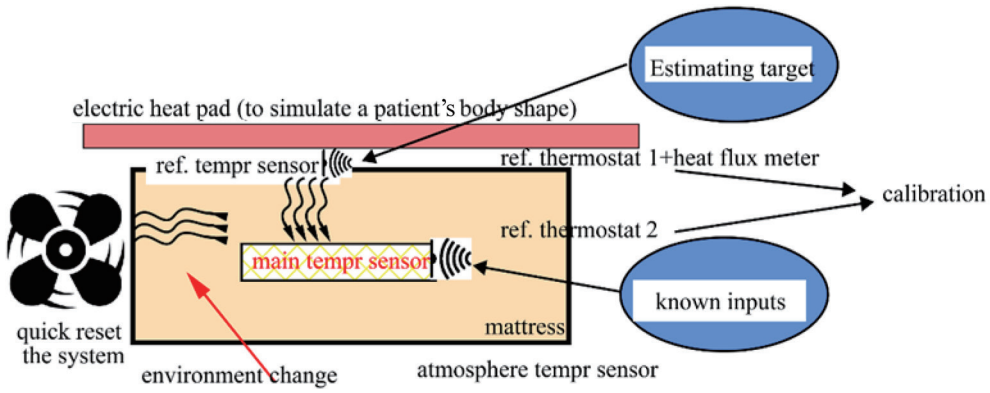

Fig. 1. (Color online) Experimental setup used in this study.

platform. The model also includes observable measured vectors and the internal state of unobservable processes that can be contaminated by noise. The POMP can be considered a generalization of a hybrid model. The hidden or potential variables that control the composition of the mixture selected in each observation are related by the Markov process rather than being independent of each other. The characteristics of the internal Markov process can be a transition density distribution, and images from internal states to external observations can be specified by measuring density distributions. We focus on Monte Carlo statistics, in which processes and noise are nonlinear and non-Gaussian.

The iterative filtering algorithm is based on the importance of the iteration sampling and maximizes the POMP as a possibility function. The algorithm solves the recursive sequence of filtering problems and merges parameters recursively when subjected to disturbances using potential variable refactoring. The iteration traverses all the possibilities on an increasingly local scale to search for the largest probability function. We set the internal state $\{X(t), t \in T)\}$ as a Markov process at time t in the time set T and write $X_{0:N} = (X_0, ..., X_N) = (X(t_0), ..., X(t_N))$ and observation $Y_{1:N} = (Y_1, ..., Y_N)$.

We assume that $X_{0:N}$ and $Y_{1:N}$ have a joint density $f_{X_{0:N}Y_{1:N}}(x_{0:N}, y_{1:N}; \theta)$ for the POMP model specified by the initial marginal density $f_{X_0}(x_0;\theta)$, the conditional transition density $f_{X_n|X_{n-1}}(x_n|x_{n-1}; \theta)$, $1 \le n \le N$, the observation process $f_{Y_n|Y_{1:n-1},X_{0:n}}(y_n \mid y_{1:n-1}, x_{0:n};\theta) = f_{Y_n|X_n}(y_n \mid x_n;\theta)$, and a series of observations denoted by $y^*_{1:N} = (y^*_1, ..., y^*_N)$.

We define the log possibility function $l_n(\theta) = \log f_Y(y^*;\theta) = \log \int f_{X_0}(x_0;\theta) \prod_{k=1}^{n} f_{X_k,Y_k|X_{k-1}}(x_k, y^*_k \mid x_{x-1};\theta) dx_{0:n}$, $1 \le n \le N$. We use an iterative filter with the aim of providing an effective and feasible algorithm to solve the problem by solving $\hat{\theta} = \arg\max_{\theta} l_N(\theta)$.

The experiments are designed as shown in Figs. 1 and 2. The main temperature sensors are placed in the center of the mattress. Then, an adjustable heating mattress is used to generate

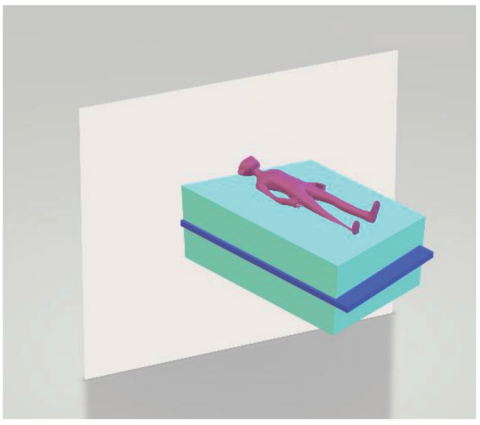

Fig. 2. (Color online) Human body lying on the surface of the mattress. Temperature sensors are installed in the center of the mattress; accordingly, the human body will not feel uncomfortable, and the complete contact temperature profile of the whole body can be measured.

a controlled source of heat on the surface of the mattress. The other side of the mattress is exposed to air to keep it at room temperature. An electric fan is installed to dissipate the accumulated heat from the previous experiment to quickly restore the starting state of the mattress so that each experiment can proceed from an equal starting temperature. In addition, we install a temperature sensor at the position required for the algorithm, that is, the surface of the mattress, to verify the results and the accuracy of the experiment.

The main aim of our research is to develop an embedded plane thermometer, as shown in Fig. 2. The human body lies on the surface of the mattress, while the temperature sensor is stored in the center of the mattress. On the one hand, this arrangement ensures that the human body will not feel uncomfortable by lying on hard objects. On the other hand, this arrangement allows the use of a few single-point thermometers to measure the complete temperature profile of the whole body at the contact surface.

3. Results

As shown in Fig. 3(a), heat from the surface of the human body flows to the middle layer of the mattress. We attach a series of thermometers to the middle layer of the mattress to measure the point temperature during the diffusion, as shown in Fig. 3(b). Our estimation method can be used to reveal the planar flux of the heating source based on the point temperature recorded in the middle layer.

To verify our algorithm, the first experiment starts with a simple setup under the assumption that the mattress is a 1D vertical line (a rod) from the surface to the bottom of the mattress. In the first experiment, we also know the thermal conductivity of the mattress. The coordinates of the line in Fig. 4 are set to 0 at the surface and 1 at the bottom of the mattress. As shown in

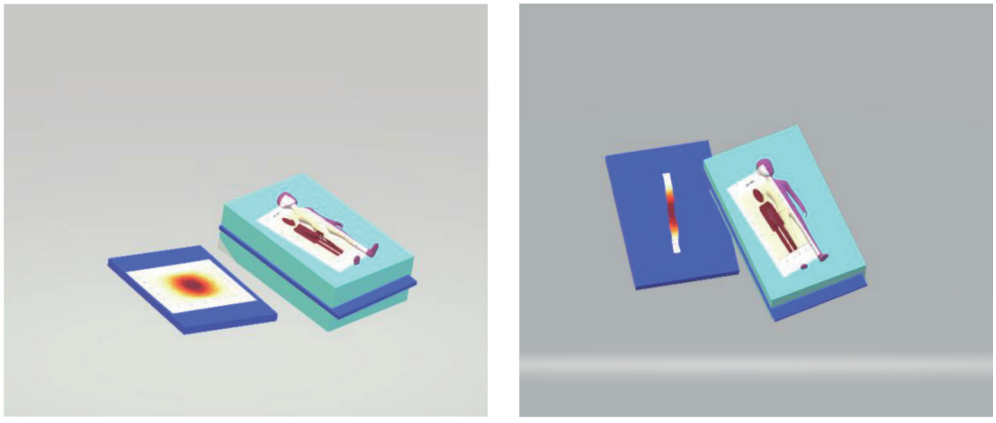

(a) (b)

Fig. 3. (Color online) (a) Heat of human body diffusing to the entire mattress. The middle layer of the mattress has a heat diffusion pattern. (b) Several thermometers are attached along the central line of the mattress to measure the temperature of the middle layer. With our estimation method, the planar thermal flow of the source can be reconstructed from the point measurements in the middle layer.

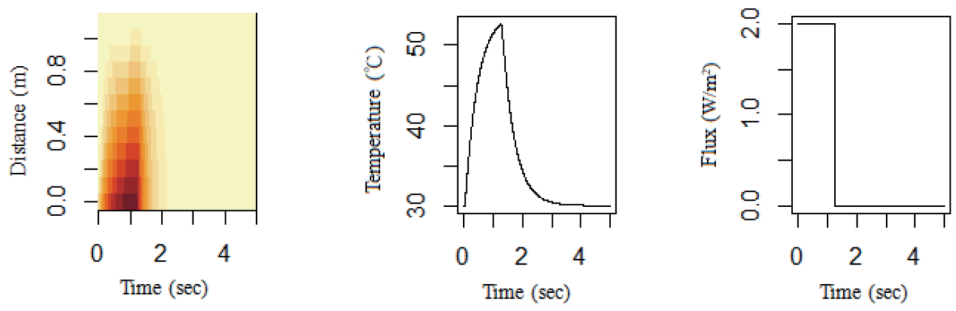

Fig. 4. (Color online) Experiment 1: center temperature and surface heat flux of a line object (a rod) that is heated for 1 s. We applied the heat flux in (c) to obtain the temperature response (b) at location 0 of the line. The heat map in (a) shows the temperature response at every location on the line from 0 to 1.

Fig. 4(c), the heat source provides heat at a rate of 2 W/m^2 at one end (location 0) of the rod for approximately 1 s before it is removed. As a result, the center point temperature first rises and then falls, as shown in Fig. 4(b). Figure 4(a) shows the thermal distribution of the entire line object during diffusion for 5 s. In the heat map, a dark color indicates a high temperature. The vertical axis is the spatial coordinate of the straight line.

Given heat transfer and diffusion, the temperature of the end will be higher than that at the center when the line is heated from the end. However, the equilibrium temperature tends to approach the ambient temperature when the heat source is removed.

The temperatures measured by thermometers are recorded at specific locations, as shown in Fig. 5. The blue line is the temperature trajectory measured at the end of the rod (location 0, or the surface of the mattress) and the red line is that of the middle location (0.5, or the center of the mattress). A 2 W/m^2 flux source is emitted on the surface of the rod and is turned off after 1 s; then, we measure the rise and fall of the temperature within 5 s at the end and the center of the rod. The temperature rises fastest at the surface because it is directly affected by the heat source, and the temperature in the middle layer needs some time to increase. However, the heat source drops to zero after only 1 s; thus, the heat of the entire mattress then freely diffuses to achieve thermal balance with room temperature.

Our algorithm can be used to estimate thermal conductivity and surface heat flux together, as shown in Figs. 6 and 7. In this measurement 1, with the known conductivity and heat flux as previously applied, our algorithm first estimates the entire heat distribution of the rod over the 5 s interval in Fig. 6(a) and then restores the original heat flux in Fig. 6(c) based on the temperature trajectory measured from the middle location in Fig. 6(b). The restored temperature trajectory and surface heat flux are similar to the original ones.

We next carry out an additional estimation. In experiment 2, we additionally estimate thermal conductivity. We find that the thermal conductivity in the first experiment becomes overestimated in some cases because the range of initial values is only approximated. The restored flux on the surface, as shown in Fig. 7(c), is overestimated at the beginning and the flux then accelerates to compensate the overestimation in the reverse direction to match the

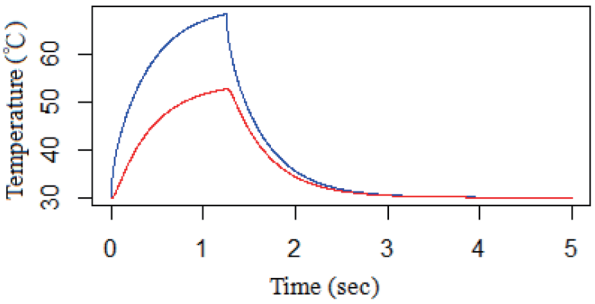

Fig. 5. (Color online) Experiment 1: temperature trajectory at two locations of the rod: end (blue) and center (red).

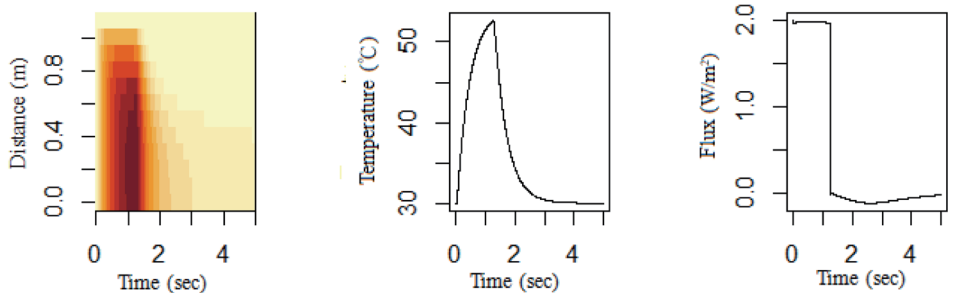

Fig. 6. (Color online) Experiment 1: estimation of the surface thermal flow of the line object with known conductivity.

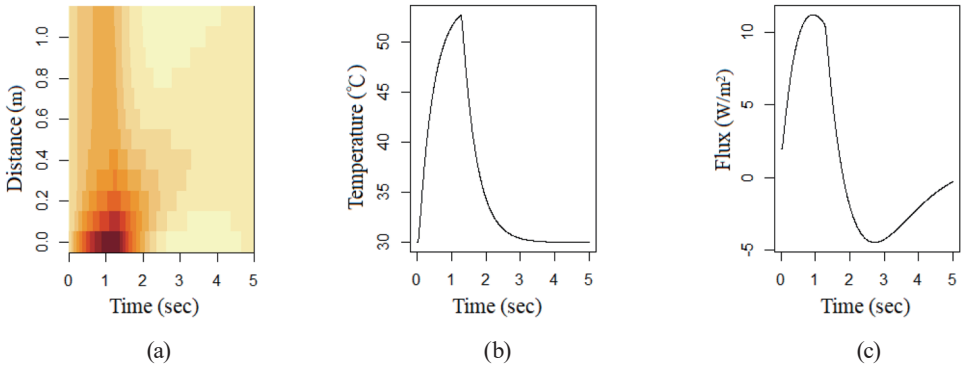

Fig. 7. (Color online) Experiment 2: estimation of the surface thermal flow and thermal conductivity of the line object. We estimate the two parameters at the same time. The explanation of subgraphs (a)–(c) is similar to that of Fig. 6.

recording at the center location. This overshoot can be made to gradually converge by our POMP correction process.

Given the heat flux previously applied, we obtain the temperature measurement in (b) at location 0.5 of the line. Using the known conductivity, we can estimate the entire heat distribution of the rod over the 5 s interval in Fig. 7(a) and estimate the heat flux at the surface shown in Fig. 7(c).

In the application to real mattresses, 3D measurement is necessary. As shown in Fig. 8, when a person lies on the surface of the mattress for 1 s, the heat flux from the human body will spread throughout the mattress. Accordingly, the temperature distribution in the entire 3D mattress will rise first and then fall. Five thermometers are installed in the middle of the mattress, as indicated in Fig. 1.

The temperature on the surface of the mattress estimated by our algorithm is shown in Fig. 9. The graph shows three snapshots of the surface temperature distribution during the diffusion process. After lying on the bed for 1 s, the person leaves the bed, and the heat will diffuse through the mattress without a heat source. When the time goes to infinity, the temperature distribution of the entire mattress will reach equilibrium with the ambient temperature.

Figure 10 shows three snapshots of the diffusion trajectory of the temperature at the middle layer of the mattress. The temperature distribution of the middle layer gradually changes from a human shape to a circular one. The speed and direction of diffusion was solved by the heat diffusion equation, and the flux on the mattress surface was well estimated.

After calculation, the restored temperature distribution and the source heat flux are similar to those of the heat source. The restored surface heat flux, as shown in Fig. 11, is also fully restored. Comparison of this with the heat source in Fig. 8 shows that the two fluxes have a similar shape and amplitude.

Fig. 8. (Color online) Experiment 3: surface heat source for a complete 3D mattress.

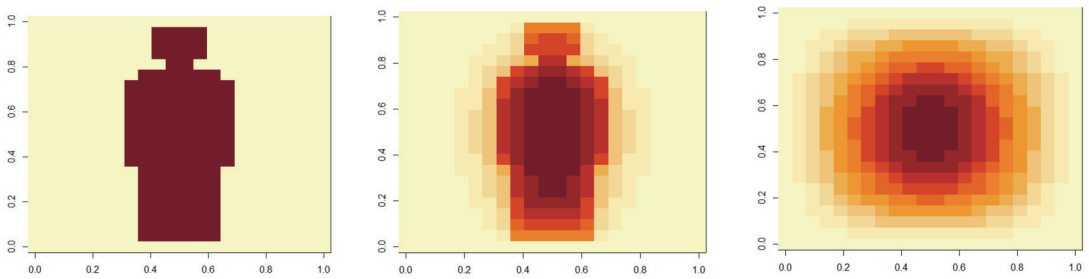

(a) (b) (c)

Fig. 9. (Color online) Experiment 3: estimated temperature distribution on the mattress *surface*: (a) at 0 s: (b) at 1 s, (c) at 2 s.

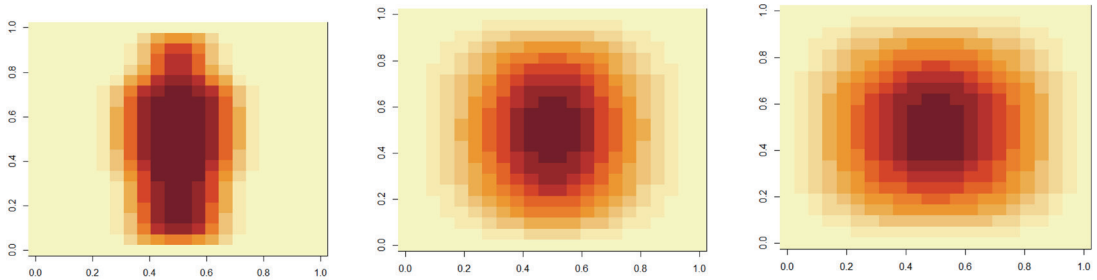

Fig. 10. (Color online) Experiment 3: estimated temperature diffusion distribution in the middle layer of the mattress: (a) at 0 s, (b) at 1 s, (c) at 2 s.

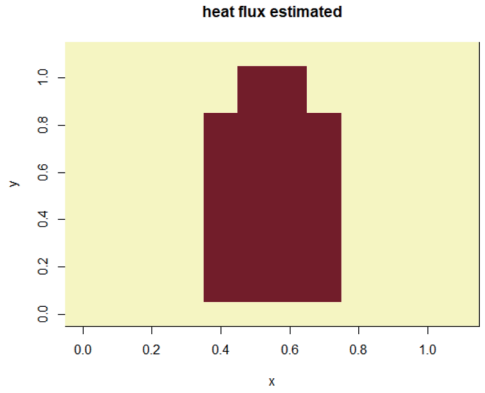

Fig. 11. (Color online) Experiment 3: reconstructed temperature distribution of the surface heat flux on the mattress.

4. Conclusions

The development of a method of mattress surface temperature estimation has the following benefits. Temperature monitoring can provide highly useful information to prevent pressure sores. (A) The large area of the planar temperature display can provide a whole view for careers. (B) The display of the heat flux generated by body contact can be directly associated with the yield of pressure sores. Thus, the method can be used to reduce the labor required to care for patients.

Our algorithm is shown to be pragmatic because the heat flux can be measured without knowing the dimensions or thermal properties of the mattress. The system can also be combined with an Internet of Things architecture to transmit the temperature and humidity to a distant caregiver via the Internet. Thus, family members who are not present can also be well-informed of the care of elderly relatives. Our result can help prevent the development of pressure sores in long-term bedridden people in addition to reducing skin damage. This will also reduce the physical and mental fatigue of caregivers and also decrease the financial burden on families.

Acknowledgments

This work was supported by the Ministry of Science and Technology, Taiwan, under grants MOST 106-2218-E-992-302-MY3, 107-2410-H-992-014-MY2, 108-2221-E-037-007, and 108-2218-E-992-304; the National Sun Yat-Sen University-Kaohsiung Medical University (NSYSU-KMU) joint research project (NSYSUKMU 109-P011); Yuan's General Hospital (YUAN-IACR-19-24, ST107007); and the Intelligent Manufacturing Research Center (iMRC) from the Featured Areas Research Center Program within the framework of the Higher Education Sprout Project by the Ministry of Education (MOE) in Taiwan.

References

1 F. Greensite: IEEE Trans. Biomed. Eng. **50** (2003) 1152. https://doi.org/10.1109/TBME.2003.817632
2 D. Wang, M. K. Robert, and R. J. Chris: IEEE Trans. Biomed. Eng. **57** (2010) 220. https://doi.org/10.1109/TBME.2009.2024928
3 A. F. Villaverde and R. B. Julio: J. R. Soc. Interface **11** (2014) 20130505. https://doi.org/10.1098/rsif.2013.0505
4 F. Campillo and V. Rossi: IEEE Trans. Aero. Elec. Syst. **45** (2009) 1063. https://doi.org/10.1109/TAES.2009.5259183
5 C. Andrieu, D. F. Nando, D. Arnaud, and I. J. Michael: Machine Learning **50** (2003) 5. https://link.springer.com/article/10.1023/A:1020281327116
6 C.Andrieu, D. Arnaud, and H. Roman: J. R. Stat. Soc. Series B **72** (2010) 269. https://doi.org/10.1111/j.1467-9868.2009.00736.x
7 J. Snoek, L. Hugo, and P. A. Ryan: Neural Information Processing Systems (NIPS) **25** (2012) 2951. https://papers.nips.cc/paper/4522-practical-bayesian-optimization-of-machine-learning-algorithms
8 T. Toni, W. David, S. Natalja, I. Andreas, and P. H. S. Michael: J. R. Soc. Interface **6** (2009) 187. https://doi.org/10.1098/rsif.2008.0172
9 E. L. Ionides, B. Anindya, A. Yves, and K. Aaron: Ann. Stat. **39** (2011) 1776. https://doi.org/10.1214/11-AOS886
10 E. L. Ionides, N. Dao, A. Yves, S. Stilian, and A. K. Aaron: PNAS **112** (2015) 719. https://doi.org/10.1073/pnas.1410597112
11 Y. Tao, Y. J. Chen, L. Xue, C. Xie, B. Jiang, and Y. Zhang: IEEE J. Biomed. Health Inf. **23** (2019) 2642. https://doi.org/10.1109/JBHI.2019.2891164
12 W. H. Tang, W. H. Ho, and Y. J. Chen: BioMed. Eng. Online **17** (2018) 147. https://doi.org/10.1186/s12938-018-0574-5